1. Khalid Subhi Ahmad[1], 2.. Mohamad Zoinol Abidin Abd. Aziz[2]

[1]Department of Electronic Engineering, Northern Technical University, (NTU) 41002 Mosul, Iraq
[2]Department of Telecommunication Engineering, Universiti Teknikal Malaysia Melaka, (UTeM) 76100 Melaka, Malaysia
ORCID: 1. 0000-0002-9194-4917

Pattern reconfigurable planar antenna array based on two circular defected ground structure

Abstract. *A pattern-reconfigurable dual-element microstrip antenna array based on reconfigurable two circular defected ground structures was proposed. Five switches are embedded in the two circular defected ground structures to tune the beam orientation. The proposed design able to work at two modes by selecting various combinations of the switch states. The proposed array was fabricated on a Roger board and prepared to shift the beam orientations at the working frequency of 7 GHz. Finally, one prototype of the antenna array was fabricated and tested. The simulated results illustrate that beam steered 52° while the measured beam steered 37°.*

Streszczenie. *Zaproponowano konfigurowalny dwuelementowy zestaw anten mikropaskowych oparty na rekonfigurowalnych dwóch kołowych strukturach naziemnych. Pięć przełączników jest osadzonych w dwóch okrągłych strukturach naziemnych z defektem, aby dostroić orientację wiązki. Proponowany projekt może pracować w dwóch trybach, wybierając różne kombinacje stanów przełącznika. Proponowany układ został wykonany na płycie Roger i przygotowany do zmiany orientacji wiązki przy częstotliwości roboczej 7 GHz. Wyprodukowano i przetestowano jeden prototyp układu antenowego. Symulowane wyniki pokazują, że wiązka kierowana była na 52 °, podczas gdy zmierzona wiązka na 37 °. (**Planarny układ antenowy z możliwością rekonfiguracji oparty na dwóch kołowych strukturach naziemnych z defektami**)*

Keywords: Array antenna, reconfigurable pattern, defected ground structures, radiation patterns, surface current, PAA.
Słowa kluczowe: antena, możliwość konfiguracji, wykrywanie struktury odbioru

Introduction

In recent years, pattern reconfigurable antennas (PRA) have gained increased attention because of their capability to control the orientation of radiation patterns [1], [2]. The conventional method for beam steering is a phased-antenna array (AA), where the orientations of the radiation pattern changed by modifying the phase of antennas in the AA. However, it suffers from high cost and large physical size, which limits its applications in communication systems [3]. Thus, PRA saves cost and installation space. Besides, it solves the probability of interference which increased owing to the massive number of customers in restricted operating bandwidth [4].

In the literature, PRA had investigated with different techniques. In [4], were designed the patch-loaded monopole element fed through a coplanar waveguide line. PIN switch diodes are incorporated on the slit of the coplanar waveguide to achieve reconfiguration. In [5], the antenna includes four similar arc dipoles and the PIN switches diodes, which incorporated in the reconfigurable antenna feeding network. In [6], used a dielectric resonator antenna ringed by six electromagnetic bandgap (EBG) sections. One PIN diode is used to control each EBG. In [7], used dual AA with stub-loaded structure. A varactor is inserted between the stub and the edge of the element. In [8], used microstrip AA with the aperture coupling technique. PIN diodes integrated at the L-stub for varying the length of the antenna feed line. In [9], a windmill-shaped loop element is proposed as the AA element. The antenna element has a four-port, and it capable of guidance its beam in four various orientations by the exciting single port at once. In [10], used two exponentially tapered slots as the AA element. Each element is integrated with two PIN diodes to control beam orientations. In [11], [12] proposed a feeding delay line technique by using a reconfigurable dual delay line. In [13]–[15], proposed using reconfigurable synthesized microstrip line technique. In [16]–[19] designed a radiating antenna surrounded by reconfigurable parasitic elements. In [20], proposed an AA that consisted of dual opposite slotted-microstrip elements linked via a slit line and the reconfiguration achieved by regulating the reverse voltages of two varactors integrated on the slit line. In [21], designed the AA of two similar elements. Each element

consists of a couple of layers, the planar inverted-F antenna layer and the monopole layer. The Pattern Reconfigurable, performed by changing the diodes on every shee. In [22] used dual folded coupled dipoles fed by dual baluns to achieve a front-to-back pattern. Dual PIN diodes are integrated into the baluns to convert the beam orientation to the front (+x orientation) or the back (−x orientation). In [23], [24] used orthogonal I-shaped defected ground structure. Moreover, few metamaterial techniques have been introduced recently using filtering features to obtain high antenna gain at a considerable frequency, such as split ring resonator (SRR) [25]-[27], frequency selective surface (FSS) [28]-[30] and electromagnetic bandgap (EBG) [31]-[33].

This letter displayed a pattern reconfigurable microstrip AA that capable of assisting the C-band application. The suggested patch antenna array (PAA) includes a dual inset rectangular microstrip element part and a coupled feed network at the front view, while at the back view are positioned two circular defected ground structures (2CDGS). Five switches are placed in a suitable position in the 2CDGS. The switches and the 2CDGS are utilized to observe the current distributions (CDs) during the ground plane hence generating pattern reconfiguration. By varying the status of the switches, the PAA can generate two modes. The beam can be shifted into two different angles in the yz-plane from 343° to 35° by controlling the switch's status.

In this research, the achievements of the AA were examined, and the simulated values were proved by the measurement of the manufactured PAA.

Reconfigurable PAA design:

The front view of the PAA that fabricated on a Rogers RT/Duroid 5880 substrate board with (εr = 2.2, tan σ=0.009) as given in Fig. 1 (a). The dimensions of the substrate board are (81 × 69.55) mm^2, and its thickness is 1.575 mm. The total dimensions of the inset rectangular microstrip patch were (18.3 × 13.22) mm^2, and each is separated by a spacing of 17.59 mm. The subminiature A connector (SMA)-port excitation is utilized in simulation. Computer Simulation Technique (CST) software is employed to simulate the PAA.

Fig. 1(b) displays the PAA back view, where two circular slots (C1 and C2) with biasing inserted on the ground plane. The radius of the C1 and C2 is 11 mm and 28 mm, respectively. The C1 and C2 have a width of 1 mm. The circumference of the C1 and the C2 circle are 69.12 mm and 175.93 mm, respectively. The circumference for C1 and C2 are approximate 17.6 λ_0, and 41 λ_0, respectively, of free space, of 7GHz.
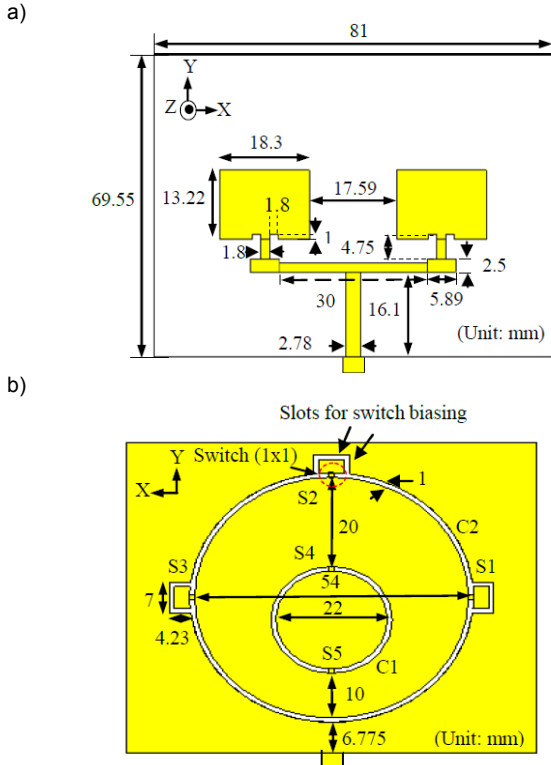
a)

b)

Fig. 1 (a) Top view of the PAA (b) 2DGS with biasing and five PIN diodes (array back view).
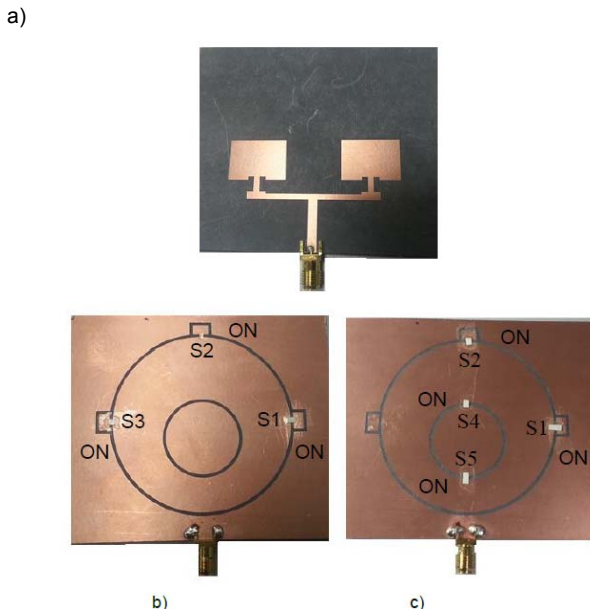
a)

Fig. 2 Photographs of the manufactured PAA (a) Top view (b) Back view Case I (c) Back view Case II.

Table 1. Switch configuration

Case	frequency	Beam angle	Switches on C2			Switches on C1	
			S1	S2	S3	S4	S5
Case I	7	343°	1	1	1	0	0
Case II	7	35°	1	1	0	1	1

1 = ON, 0 = OFF

To achieve reconfigurability, five switches connected on the 2CDGS. The copper tape is used to represent the switch. While, in the simulation, the switch is symbolized by the copper bridge.

Fig.2 illustrates the manufactured PAA, and Table 1 shows the switch configuration of the PAA.

In this research, the copper tape is used as the ideal switch for reconfigurability based on the proof of approach [34], [35]. The absence of the copper tape represents that the switch in the OFF state. The presence of the tape symbolizes that switch in the ON state.

Empirical results:

Fig. 3 (a) presents the simulated surface CDs (J[A/m]) at the working frequency of 7 GHz for Case I. It was seen that most of the CDs around the switches on the C2 in ON state (S1, S2, S3). In spite of the switches on the C1 in OFF state but it observed higher CDs on the upper right and left side of the C1.

Fig. 3 (b) presents CDs in Case II. the CDs are higher around the C1 due to the switches S4 and S5 are in ON state. While the CDs around switches S1 and S2 lower, but due to the S1 and S2 are in ON state, the CDs are higher around the lower left side of the C2.
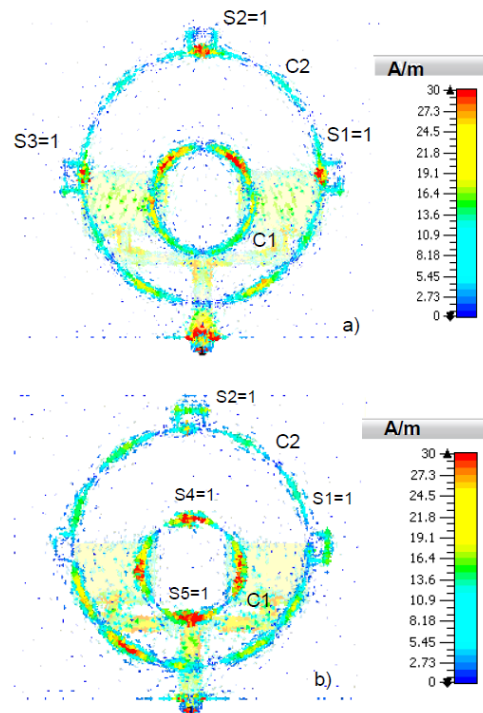

Fig. 3 Simulated surface CDs on the ground portion. (a) Case I (b) Case II.

Fig.4 (a) and (b) illustrate the far-field radiation patterns in (yz- plane) at 7 GHz, cases I and II, respectively. In Case I, the radiation pattern orientation is steered to Θ = 343° at 7.84 dBi versus side lobe gain of -4.1 dB. In Case II, a considerable variation in the beam orientation is observed at Θ = 35°, with a decrease in the gain to 7.14 dBi and the sidelobe gain of −3.1 dB, as illustrated in Table 2. Fig.5 depicts the comparison of the simulated radiation patterns between cases I and II at 7 GHz, in E-plane and H-plane.

Table 2. Beam orientation ability for Case I and Case II

Array Type	Gain (dBi)	Main Lobe Orientation	Side Lobe (dB)
Case I	7.84	343°	-4.1
Case II	7.14	35°	-3.1

7.84 dBi

Θ =343°

dBi

7.84
5.39
3.92
2.45
0.98
-1.07
-4.29
-7.51
-10.7
-13.9
-17.2

a)

7.15 dBi

Θ =35°

dBi

7.15
4.91
3.57
2.23
0.893
-1.12
-4.46
-7.81
-11.2
-14.5
-17.9

b)
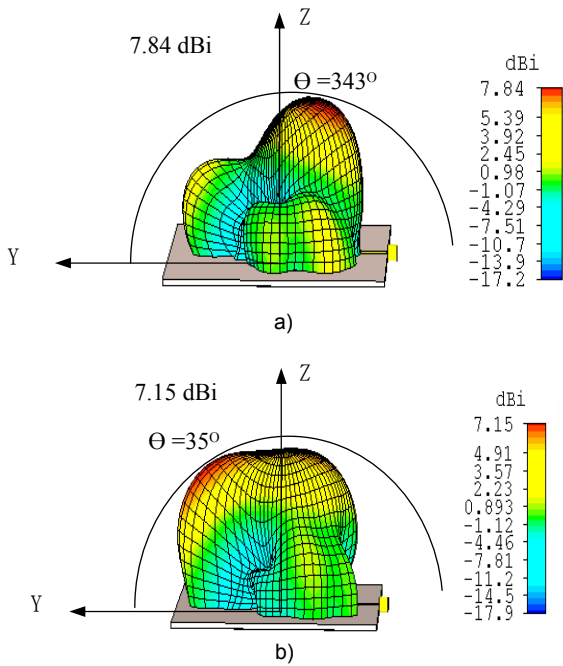
Fig. 4 Simulated 3-D radiation pattern at 7GHz (a) Case I (b) Case II.

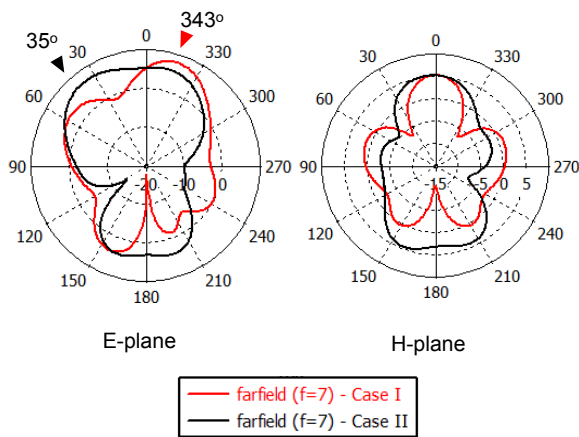

E-plane

H-plane

farfield (f=7) - Case I
farfield (f=7) - Case II

Fig. 5 Radiation patterns comparison between Case I and II on E-plane and H-plane at 7 GHz.

Fig. 6 (a) compares the measured and the simulated reflection losses of the PAA for Case I. The -10 dB reflection loss defines the simulated bandwidth (BW) is 190 MHz (6.45-6.64) GHz and 560 MHz (6.91-7.47) GHz, and the measured BW is 950 MHz (6.66-7.61) GHz. Fig. 6 (b) compares the measured and the simulated reflection losses of the PAA for Case II. The -10 dB reflection loss defines the simulated BW is 1050 MHz (6.46-7.51) GHz, and the measured BW is 1080 MHz (6.54-7.62) GHz. The inaccuracies in manufacturing have reasoned the variations between the results measured and those simulated; however, in general, they are in good acceptance.
Fig. 6 shows that the reflection loss operating frequency 7 GHz is below 10 dB in Case I and II.

The measurement and the far-field simulation patterns in both E-plane and H-plane at Case I and Case II were normalized and illustrated in Fig. 7 and 8, respectively. The simulated beam steered 52° from 343° to 35° while the measured beam steered 37° from 353° to 30°. The results indicate acceptable agreement in both.
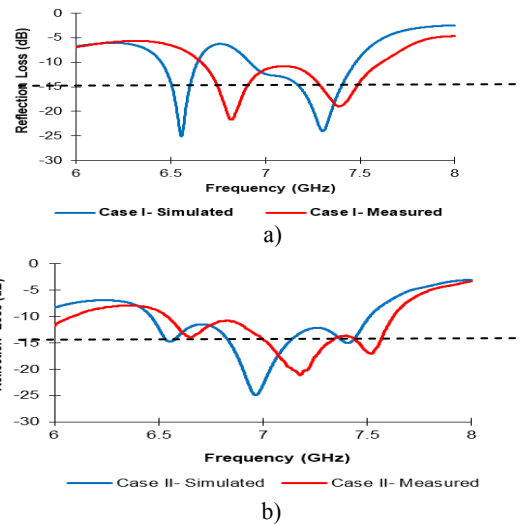

a)

b)

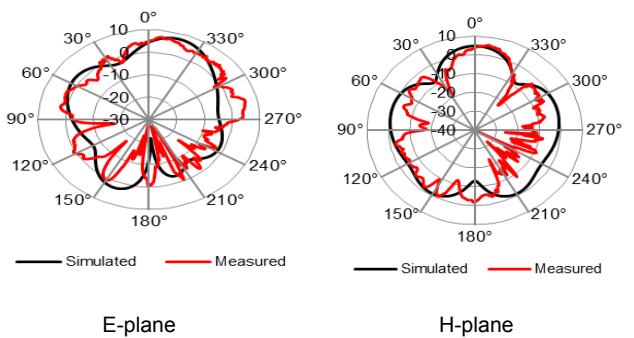Fig. 6 Reflection losses comparison simulated and measured (a) Case I (b) Case II.

E-plane

H-plane

Fig. 7 Measured and simulated radiation patterns for E-plane and H-plane, Case-1 at 7 GHz.
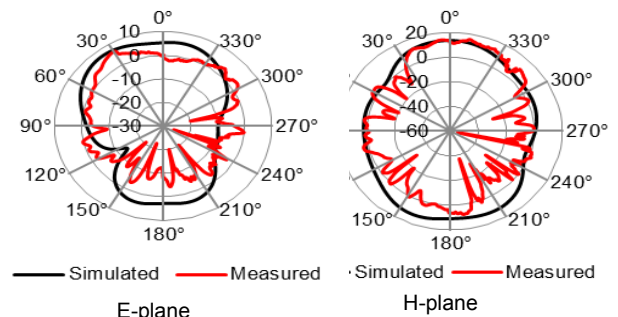

E-plane

H-plane

Fig. 8 Measured and predicted Far field patterns for E-plane and H-plane, Case-II at 7 GHz.

Conclusion:
In this paper, the beam-shifting technique utilizing a planar AA with a 2CDGS was simulated, fabricated, and investigated. The measurement outcomes confirmed that the PAA could shift the beam across 353° and 30° in E-plane. The proposed antenna can be further used for Ultrawideband application in the future [36].

Authors: The first author name is Khalid Subhi Ahmad, from the Mosul Technical Institute, Northern Technical University, (NTU) 41002 Mosul, Iraq, email: jarkovo_1988@ntu.edu.com. The second author name is Mohamad Zoinol Abidin Abd. Aziz, from the Faculty of Electronics and Computer Engineering, Universiti Teknikal Malaysia Melaka (UTeM), Jalan Hang Tuah Jaya, 76100 Durian Tunggal, Melaka. email:mohamadzoinol@utem.edu.my.

REFERENCES

[1] H. W. Deng, T. Xu, and F. Liu, Broadband Pattern-Reconfigurable Filtering Microstrip Antenna with Quasi-Yagi Structure,*IEEE Antennas Wirel. Propag. Lett.*, vol.17, no.7, pp. 1127–1131, 2018.

[2] W. Lin, H. Wong, and R. W. Ziolkowski, Wideband Pattern-Reconfigurable Antenna with Switchable Broadside and Conical Beams,*IEEE Antennas Wirel. Propag. Lett.*, vol.16, no. c, pp. 2638–2641, 2017.

[3] Khalid Subhi Ahmad, Fauziahanim Che Seman, Shipun Anuar Hamzah, Goh Chin Hock, and Shaharil Mohd Shah, Circuit Model for Microstrip Array Antenna with Defected Ground Structures for Mutual Coupling Reduction and Beamforming Applications, *Int. J. of Integrated Eng.*, vol. 13, no. 1, pp. 101-119, 2021.

[4] I. Lim, and S. Lim, Monopole-Like and Boresight Pattern Reconfigurable Antenna, *IEEE Trans. Antennas Propag.*,vol. 61, no. 12, pp. 5854–5859, 2013.

[5] G. Jin, M. Li, D. Liu, and G. Zeng, A Simple Planar Pattern-Reconfigurable Antenna Based on Arc Dipoles, *IEEE Antennas Wirel. Propag. Lett.*, vol. 17, no. 9, pp. 1664–1668, 2018.

[6] A. R. S. I. Ben Mabrouk, M. Al-Hasan, M. Nedil, and T. A. Denidni, A Novel Design of Radiation Pattern-Reconfigurable Antenna System for Millimeter-Wave 5G Applications, *IEEE Trans. Antennas Propag.*, vol. 68, no. 4, pp. 2585-2592, 2019.

[7] S. N. M. Zainarry, N. Nguyen-Trong, and C. Fumeaux, A Frequency- and Pattern-Reconfigurable Two-Element Array Antenna, *IEEE Antennas Wirel. Propag. Lett.*, vol.17, no. 4, pp. 617–620, 2018.

[8] N. Ramli, M. T. Ali, M. T. Islam, A. L. Yusof, and S. Muhamud-Kayat, Aperture-Coupled Frequency and Patterns Reconfigurable Microstrip Stacked Array Antenna, *IEEE Trans. Antennas Propag.*, vol. 63, no. 3, pp. 1067–1074, 2015.

[9] Y. F. Cheng, X. Ding, W. Shao, and B. Z. Wang, Planar Wide-Angle Scanning Phased Array with Pattern-Reconfigurable Windmill-Shaped Loop Elements*, IEEE Trans. Antennas Propag.*, vol. 65, no. 2, pp. 932–936,2017, doi : 10.1109/TAP.2016.2632736.

[10] Z. Jiang, S. Xiao, and Y. Li, A Wide-Angle Time-Domain Electronically Scanned Array Based on Energy-Pattern-Reconfigurable Elements, *IEEE Antennas Wirel. Propag. Lett.*, vol. 17, no. 9, pp. 1598–1602, 2018.

[11] X. G. Zhang, W. X. Jiang, H. W. Tian, Z. X. Wang, Q. Wang, and T. J. Cui, Pattern-Reconfigurable Planar Array Antenna Characterized by Digital Coding Method, *IEEE Trans. Antennas Propag.*,vol. 68, no. 2, pp. 1170-1175., 2019.

[12] M. A. Aris, M. T. Ali, N. H. Abd Rahman, and I. Pasya, Radiation Pattern Reconfigurable Microstrip Patch Antenna using Dual Delay Line*, J. Teknol.*, vol. 80, no. 1, pp. 9–16, 2018.

[13] H. N. Chu, G. Y. Li, and T. G. Ma, Planar Pattern Switchable Antenna using Phase Reconfigurable Synthesized Transmission Lines, *IEEE Antennas Wirel. Propag. Lett.*, vol. 17, no. 12, pp. 2319–2323, 2018.

[14] J. Y. Zou, C. H. Wu, and T. G. Ma, Heterogeneous Integrated beam-switching/Retrodirective Array using Synthesized Transmission Lines*, IEEE Trans. Microw. Theory Tech.*, vol. 61, no. 8, pp. 3128–3139, 2013.

[15] H. N. Chu, and T. G. Ma, Beamwidth Switchable Planar Microstrip Series-Fed Slot Array using Reconfigurable Synthesized Transmission Lines, *IEEE Trans. Antennas Propag.*, vol. 65, no. 7, pp. 3766–3771, 2017.

[16] P. Lotfi, S. Soltani, and R. D. Murch, Broadside Beam-Steerable Planar Parasitic Pixel Patch Antenna, *IEEE Trans. Antennas Propag.*, vol. 64, no. 10, pp. 4519– 4524, 2016.

[17] L. Yang, C. Lu, X. Li, L. Liu, and X. Yin, A horizontal Azimuth Pattern-Reconfigurable Antenna using Omnidirectional Microstrip Arrays for WLAN Application*, Int. J. Antennas Propag.*, vol. 2019.

[18] Y. Zhang, S. Lin, S. Yu, G. J. Liu, and A. Denisov, Design and Analysis of Optically Controlled Pattern Reconfigurable Planar Yagi-Uda Antenna*, IET Microwaves, Antennas Propag.*, vol. 12, no. 13, pp. 2053–2059, 2018.

[19] S. L. Chen, P. Y. Qin, W. Lin, and Y. J. Guo, Pattern-Reconfigurable Antenna with Five Switchable Beams in Elevation Plane, *IEEE Antennas Wirel. Propag. Lett.*, vol. 17, no. 3, pp. 454–457, 2018.

[20] J. S. Row, and Y. H. Wu, Pattern Reconfigurable Slotted-Patch Array, *IEEE Trans. Antennas Propag.*, vol. 66, no. 3, pp. 1580–1583, 2018.

[21] H. Li, B. K. Lau, and S. He, Design of Closely Packed Pattern Reconfigurable Antenna Array for MIMO Terminals, *IEEE Trans. Antennas Propag.*, vol. 65, no. 9, pp. 4891–4896, 2017.

[22] R. Li, H. Yang, B. Liu, Y. Qin, and Y. Cui, Theory and Realization of a Pattern-Reconfigurable Antenna Based on Two Dipoles, *IEEE Antennas Wirel. Propag. Lett.*, vol. 17, no. 7, pp. 1291–1295, 2018.

[23] K. S. Ahmad, F. C. Seman, and S. A. Hamzah, Beam Steering of Array Antenna with 2-orthogonal-I-Shaped Defected Ground Structure, *IEEE Asia-Pacific Conference on Applied Electromagnetics*, APACE, pp. 296-300, 2016.

[24] K. S. Ahmad, F. C. Seman, and S. A. Hamzah, Dual Microstrip Antenna Patches with Orthogonal I-Shaped Defected Ground Structure for Beam Steering Realization, *IEEE Asia-Pacific Conference on Applied Electromagnetics*, APACE, pp. 174-178, 2016.

[25] M. Ibrahim, A. J. A. Al-gburi, Z. Zakaria, and H. A. Bakar, "Parametric Study of Modified U-shaped Split Ring Resonator Structure Dimension at Ultra-Wide-band Monopole Antenna," *J. Telecommun. Electron. Comput. Eng.*, vol. 10, no. 2, pp. 53–57, 2018.

[26] A. J. A. Al-Gburi, I. M. Ibrahim, and Z. Zakaria, "Band-notch effect of U-shaped split ring resonator structure at ultra wide-band monopole antenna," *Int. J. Appl. Eng. Res.*, vol. 12, no. 15, pp. 4782–4789, 2017.

[27] M. Y. Zeain, M. Abu, A. J. A. Al-gburi, Z. Zakaria, R. Syahputri, and A. Toding, "Design of a wideband strip helical antenna for 5G applications," *Bull. Electr. Eng. Informatics*, vol. 9, no. 5, pp. 1958–1963, 2020.

[28] A. J. A. Al-gburi, I. M. Ibrahim, M. Y. Zeain, and Z. Zakaria, "Compact Size and High Gain of CPW-fed UWB Strawberry Artistic shaped Printed Monopole Antennas using FSS Single Layer Reflector," *IEEE Access*, vol. 8, no. 5, pp. 92697–92707, 2020.

[29] A. J. A. Al-gburi *et al.*, "A compact UWB FSS single layer with stopband properties for shielding applications," *Przegląd Elektrotechniczny*, no. 2, pp. 167–170, 2021.

[30] H. H. Keriee *et al.*, "High gain antenna at 915 mhz for off grid wireless networks," *Bull. Electr. Eng. Informatics*, vol. 9, no. 6, pp. 2449–2454, 2020.

[31] A. J. Abdullah Al-Gburi, I. M. Ibrahim, Z. Zakaria, and A. D. Khaleel, "Gain Improvement and Bandwidth Extension of Ultra-Wide Band Micro-Strip Patch Antenna Using Electromagnetic Band Gap Slots and Superstrate Techniques," *J. Comput. Theor. Nanosci.*, vol. 17, no. 2–3, pp. 985–989, 2020.

[32] A. J. A. Al-Gburi, I. Ibrahim, and Z. Zakaria, "Gain Enhancement for Whole Ultra-Wideband Frequencies of a Microstrip Patch Antenna," *J. Comput. Theor. Nanosci.*, vol. 17, no. 2–3, pp. 1469–1473, 2020.

[33] M. Y. Zeain *et al.*, "Design of helical antenna for next generation wireless communication," *Prz. Elektrotechniczny*, no. 11, pp. 96–99, 2020.

[34] H. B. El-Shaarawy, F. Coccetti, R. Plana, M. El-Said, and E. A. Hashish, Novel Reconfigurable Defected Ground Structure Resonator on Coplanar Waveguide, *IEEE Trans. Antennas Propag.*, vol. 58, no. 11, pp. 3622–3628, 2010.

[35] N. AL-Fadhali, H. Majid, and R. Omar, Multiband Frequency Reconfigurable Substrate Integrated Waveguide Antenna using Copper Strip for Cognitive Radio Applicable to Internet of Things Application, *Telecommun. Syst.*, vol. 76, issue 3, pp. 345–358, 2020.

[36] A. J. A. Al-gburi et al., "High Gain of UWB CPW-fed Mercedes-Shaped Printed Monopole Antennas for UWB Applications," *Prz. Elektrotechniczny*, no. 5, pp. 70–73, 2021.